Published in final edited form as:

Chem Commun (Camb). 2015 August 11; 51(62): 12439–12442. doi:10.1039/c5cc04545b.

[^{18}F]–NHC–BF_3 adducts as water stable radio-prosthetic groups for PET imaging†,„‡

Kantapat Chansaenpak[a,§], **Mengzhe Wang**[b,§], **Zhanhong Wu**[b], **Rehmat Zaman**[a], **Zibo Li**[b,¶], and **François P. Gabbaï**[a,¶]

[a]Department of Chemistry, Texas A&M University, College Station, Texas 77843, USA

[b]Department of Radiology, Biomedical Research Imaging Center, University of North Carolina, Chapel Hill 27599, USA

Abstract

The radiofluorination of N-heterocyclic carbene (NHC) boron trifluoride adducts affords novel [^{18}F]–positron emission tomography probes which resist hydrolytic fluoride release. The labelling protocol relies on an ^{18}F–^{19}F isotopic exchange reaction promoted by the Lewis acid $SnCl_4$. Modification of the NHC backbone with a maleimide functionality provides access to a model peptide conjugate which shows no evidence of defluorination when imaged *in vivo*.

Positron emission tomography (PET) is a rapidly growing imaging technique that relies on the use of molecular radiotracers containing a positron emitting isotope.[1] To date, a great deal of attention has been devoted to the use of fluorine-18 (^{18}F), a radionuclide that can be easily generated from [^{18}O]–water and whose nuclear decay characteristics are ideally suited for applications in PET imaging.[2] One difficulty faced in the synthesis of ^{18}F-containing molecular radiotracers is the short half-life of the isotope (110min). It follows that the best methods to access ^{18}F-containing molecular radiotracers should be fast and preferably carried out in the late stages of the synthesis of the radiopharmaceutical probe.[3] An attractive approach that provides a possible solution to these challenges is based on molecules containing a boron atom as a fluoride binding site.[4] This approach was pioneered by Perrin who showed that arylboronic acids or esters featuring electron-withdrawing groups quickly react with fluoride ions to form the corresponding aryltrifluoroborates.[5] Over the years, Perrin and other groups have investigated a number of backbones designed to stabilize the trifluoroborate unit and prevent its decomposition *in vivo* (Chart 1).[6] Although the rate of hydrolysis can be slowed down drastically, all fluoroborates investigated to date are unstable toward hydrolysis. This hydrolysis reaction is potentially problematic because the fluoride ions liberated by hydrolysis of the radiotracer lead to unwanted background signal in particular from the skeleton.

†This work is dedicated to Manfred Scheer on the occasion of his 60th birthday.

‡Electronic supplementary information (ESI) available: Experimental, characterization and imaging data. CCDC 1402916–1402918. For ESI and crystallographic data in CIF or other electronic format see DOI: 10.1039/c5cc04545b

Correspondence to: Zibo Li; François P. Gabbaï.

§Contributed equally to the work.

¶Jointly conceived the study.

Recently we introduced a strategy based on the use of zwitterionic trifluoroborates.[6f,g] In particular, we found that the trifluoroborate moiety can be significantly stabilized against hydrolysis by a proximal cationic functionality such as a phosphonium unit as in the case of **D** and **E**.[6g] This approach is further validated by the recent work of Perrin who showed that ammonium trifluoroborate moieties of type **C** show sufficient stability for *in vivo* imaging.[6b,c] As part of our continuing interest in this chemistry, we were drawn by the remarkable stability of N-heterocyclic carbene (NHC) boron fluoride adducts[7] such as **1**.[8] Compound **1**, which can also be described as a zwitterionic imidazolium trifluoroborate is highly resistant to hydrolysis and can be recrystallized from boiling water. Encouraged by these properties, we questioned whether such NHC–BF_3 adducts could be radiofluorinated and used as prosthetic groups for PET imaging. In this paper, we describe the initial results that we have obtained while working toward this goal.

As a starting point for these studies, we synthesized the carbene–BF_3 adduct **2** as a model compound. Using the method recently employed by for the monoethyl analog (**1**),[8] compound **2** was obtained by thermolysis of 1,3-dimethyl-1*H*-imidazolium tetrafluoroborate under reduced pressure (Scheme 1).[8] The presence of the trifluoroborate moiety is confirmed by the detection of a quartet in both the ^{11}B NMR spectrum (0.21 ppm, $J_{B–F}$ = 37.0 Hz) and the ^{19}F NMR spectrum (−139.2 ppm, $J_{B–F}$ = 37.0 Hz). The ^{1}H NMR spectrum shows two singlets at 3.85 ppm and 7.11 ppm corresponding to the methyl and the methine groups, respectively. The structure of this compound has also been studied by single crystal X-ray diffraction (Fig. 1). The B(1)–C(1) bond connecting the NHC ligand to the boron center (1.641(3) Å) is comparable to the boron–carbon bond of **1** (1.644(3) Å),[8] indicating a strong coordination of the NHC ligand to the boron atom.

Next, we turned our attention toward the synthesis of a NHC–BF_3 adduct that could be easily conjugated with biomolecules for targeted disease imaging. After reviewing different functionalization possibilities, we decided to synthesize the amino-substituted derivative **5** (Scheme 2). We successfully accessed this new derivative by reaction of the known nitrocarbene–AgI complex **3**[9] with BF_3–OEt_2. This reaction afforded the nitrocarbene–BF_3 adduct **4** as a white solid in 83% yield. Hydrogenation of **4** over palladium afforded **5** in a 78%yield. The ^{1}H NMR spectrum of **4** and **5** display two singlets (3.94 ppm and 4.16 ppm for **4** and 3.61 and 3.73 ppm for **5**) corresponding to themethyl group and a singlet (8.21 ppm for **4** and 6.37 ppm for **5**) corresponding to the methine proton. The presence of an amino group in **5** is confirmed by the detection of a broad signal at 4.02 ppm. As in the case of **2**, quartets are observed in the ^{11}B NMR and ^{19}F NMR spectra of **4** and **5** (^{11}B NMR: 0.13 ppm, $J_{B–F}$ = 33.5 Hz for **4** and 0.27 ppm, $J_{B–F}$ = 37.2 Hz for **5**; ^{19}F NMR: −137.9 ppm, $J_{B–F}$ = 33.5 Hz for **4** and −138.0 ppm, $J_{B–F}$ = 37.2 Hz for **5**). The crystal structure of **4** has also been determined. The carbene–BF_3 moiety is essentially analogous to that in **2** (Fig. 1). The only notable difference is observed in the B(1)–C(1) separation (1.657(2) Å) which is slightly longer than in **2** (1.637(5) Å). This elongation is assigned to the electron withdrawing properties of the nitro group and the associated weaker donor properties of the carbene–carbon atom.

Compound **5** can be easily converted into the maleimide derivative **7** in two steps as illustrated in Scheme 2. The spectroscopic properties of **7** are close to those of **5**. The methine signal is observed at 7.08 ppm. The trifluoroborate moiety gives rise to a quartet at 0.29 ppm in the ^{11}B NMR spectrum($J_{B–F}$ = 35.6 Hz) as well as a quartet at −138.5 ppm in the ^{19}F NMR spectrum($J_{B–F}$ = 35.6 Hz). The structure of this derivative has also been confirmed by X-ray diffraction (Fig. 1). The B(1)–C(1) separation (1.656(9) Å) is close to that in **4**, a characteristic consistent with the electron withdrawing properties of the maleimide functional group.

Next, we decided to investigate the rates of hydrolysis of these new NHC–BF_3 adducts (**2**, **4**, **5**, **7**). This hydrolysis reaction, which is expected to produce the corresponding boronic acid according to a first order rate process ($\nu = k_{obs}$[NHC–BF_3]), was monitored by ^{19}F NMR spectroscopy in D_2O/CD_3CN (8/2 vol) at pH 7.5 ([phosphate buffer] = 500 mM, [NHC–BF_3] = 20 mM).[4d,10] Surprisingly, we found that the hydrolysis of the adducts was extremely slow. After a week, we did not observe any free fluoride for **4** and **7** indicating that these two derivatives are essentially immortal. Their stability is assigned to the electron withdrawing nature of the nitro or maleimide functionality which increases the Lewis acidity of the boron center thereby preventing fluoride anion dissociation. Compounds **2** and **5** are also surprisingly stable and only show a trace amount of free fluoride after a week in D_2O/CD_3CN (8/2 vol) at pH 7.5. By extending this experiment to a longer timescale, we have been able to calculate the rate of hydrolysis for these two compounds. These rates, which are respectively equal to $k_{obs} = 1.2 \times 10^{-6}$ min^{-1} for **2** and 1.1×10^{-6} for **5** are lower than those measured under the same conditions for the phosphonium borane **D**. Altogether, these results illustrate the remarkable resistance of NHC–BF_3 adducts to hydrolysis and suggest that they could be used as prosthetic groups for PET imaging.

Employing the approach developed by our group for the preparation of [^{18}F]BODIPY dyes,[11] we decided to investigate the radiofluorination of these NHC–BF_3 adducts *via* ^{18}F–^{19}F isotopic exchange using $SnCl_4$ as a Lewis acid promoter. We first tested this approach with the non-functionalized NHC–BF_3 adduct **2** which was mixed with $SnCl_4$ (5–15 eq.) in MeCN and combined with a solution of [^{18}F]–fluoride (as the tetra-*n*-butylammonium salt) in MeCN (Scheme 3 and Table 1). The reaction mixture was then shaken for 10 min before being quenched by addition of water. The radiolabeled compound ([^{18}F]**2**) was immobilized on a Sep-Pak cartridge (Sep-Pak Plus tC18) and washed with water. [^{18}F]**2** was eluted off the cartridge with MeCN. An aliquot of the resulting MeCN solution was subjected to HPLC analysis.

The radiochemical yield (RCY) was calculated based on the radio-activity of the isolated product and the starting radio-activity. As shown in Table 1, the RCY ranges from 35–56% for different reaction conditions. It was found that increasing the concentration of precursor leads to higher isolation yield (entries 1–3). Interestingly, variation in the concentration of the Lewis acid promoter (entries 3–5) or in the temperature (entries 6 and 7) of the reaction had little impact on the RCY. When a long reaction time was employed as in entries 8 and 9, a decreased isolation yield was observed due to product decomposition. The highest specific activity of the final product obtained in this experiment was calculated to be 53.5 mCi μmol^{-1} (entry 8).

Using conditions from entry 7, we have also been able to prepare [^{18}F]**7** with a specific activity of 51.3 mCi μmol^{-1} (RCY = 54%, Scheme 4). The identity of [^{18}F]**7** was confirmed by co-injection with the non-radiolabeled standard (Fig. 2). This radiofluorinated NHC–BF_3 adduct could be conveniently conjugated with the model peptide H–Cys–Phe–OH *via* a thiol-Michael addition reaction. This synthesis was carried out by mixing a solution of [^{18}F]**7** in MeCN with an aqueous solution of H–Cys–Phe–OH (400 μg, 1.5 μmol) (Scheme 4). After shaking for 10 min at room temperature, a portion of the reaction mixture (0.01 mCi) was loaded onto the HPLC for purification affording [^{18}F]**7**–H–Cys–Phe–OH with a 95.7% purity. The identity of [^{18}F]**7**–H–Cys–Phe–OH peptide was confirmed by its mass spectrum (Fig. S11, ESI‡) as well as by co-injection with the independently synthesized non-radiolabeled standard (Fig. 3). The specific activity of [^{18}F]**7**–H–Cys–Phe–OH peptide was calculated as 40.8 mCi μmol^{-1}.

Encouraged by these radiofluorination and conjugation results, the stability of [^{18}F]**7**–H–Cys–Phe–OH was investigated *in vivo*. As a prelude to these studies, we first tested the stability of the conjugate in a 1× PBS buffer at 37 °C (Fig. S14, ESI‡). Even after 2 hours, the conjugate is not compromised as shown by the fact that its purity remains >90% pure. *In vivo* PET/CT imaging in a normal nude mouse afford consistent results. The microPET/CT images collected 1 h, 2 h, and 4 h post injection show liver and urinary track clearance of the conjugate. More importantly, no bone uptake is observed even 4 h post injections. Indicating that [^{18}F]–fluoride release by the radiofluorinated carbene unit is negligible (Fig. 4).

In summary, we have identified a new boron-based fluoride captor with an unusually high resistance to hydrolytic fluoride release. The stability of this new probe is ascribed to its zwitterionic nature, with the cationic charge of the imidazolium unit acting as an electrostatic anchor for the boron-bound fluoride anions. These NHC–BF_3 fluoride captors are a new incarnation of the concepts underlying the stability of the phosphonium trifluoroborates of type **D** and **E** developed by us or ammonium trifluoroborates of type **C** recently reported by the Perrin group.

Supplementary Material

Refer to Web version on PubMed Central for supplementary material.

Acknowledgments

This work was supported by the Cancer Prevention Research Institute of Texas (RP130604), the National Institute of Biomedical Imaging and Bioengineering (1R01EB014354-01A1), the National Cancer Institute (P30-CA016086-35-37), and the Biomedical Research Imaging Center, University of North Carolina at Chapel Hill. K.C. gratefully acknowledges financial support from the Development and Promotion of Science and Technology (DPST) program administered by the Royal Thai Government.

Notes and references

1. Miller PW, Long NJ, Vilar R, Gee AD. Angew Chem, Int Ed. 2008; 47:8998–9033.
2. (a) Dolle, F., Roeda, D., Kuhnast, B., Lasne, M-C. Fluorine-18 chemistry for molecular imaging with positron emission tomography. In: Tressaud, A., editor. Fluorine and Health. Elsevier; Amsterdam: 2008. p. 3-65.(b) Cai L, Lu S, Pike VW. Eur J Org Chem. 2008:2853–2873.

3. Bhalla R, Darby C, Levason W, Luthra SK, McRobbie G, Reid G, Sanderson G, Zhang W. Chem Sci. 2014; 5:381–391.

4. (a) Ting R, Adam MJ, Ruth TJ, Perrin DM. J Am Chem Soc. 2005; 127:13094–13095. [PubMed: 16173707] (b) Harwig CW, Ting R, Adam MJ, Ruth TJ, Perrin DM. Tetrahedron Lett. 2008; 49:3152–3156.(c) Ting R, Harwig C, auf dem Keller U, McCormick S, Austin P, Overall CM, Adam MJ, Ruth TJ, Perrin DM. J Am Chem Soc. 2008; 130:12045–12055. [PubMed: 18700764] (d) Ting R, Harwig CW, Lo J, Li Y, Adam MJ, Ruth TJ, Perrin DM. J Org Chem. 2008; 73:4662–4670. [PubMed: 18489162] (e) Ting R, Lo J, Adam MJ, Ruth TJ, Perrin DM. J Fluorine Chem. 2008; 129:349–358.(f) Li Z, Lin TP, Liu S, Huang CW, Hudnall TW, Gabbaï FP, Conti PS. Chem Commun. 2011; 47:9324–9326.(g) Hendricks JA, Keliher EJ, Wan D, Hilderbrand SA, Weissleder R, Mazitschek R. Angew Chem, Int Ed. 2012; 51:4603–4606.(h) Liu S, Li D, Shan H, Gabbaï FP, Li Z, Conti PS. Nucl Med Biol. 2014; 41:120–126. [PubMed: 24210284]

5. (a) Li Y, Asadi A, Perrin DM. J Fluorine Chem. 2009; 130:377–382.(b) auf dem Keller U, Bellac CL, Li Y, Lou Y, Lange PF, Ting R, Harwig C, Kappelhoff R, Dedhar S, Adam MJ, Ruth TJ, Bénard F, Perrin DM, Overall CM. Cancer Res. 2010; 70:7562–7569. [PubMed: 20729277] (c) Li Y, Ting R, Harwig CW, auf dKU, Bellac CL, Lange PF, Inkster JAH, Schaffer P, Adam MJ, Ruth TJ, Overall CM, Perrin DM. Med Chem Commun. 2011; 2:942–949.(d) Liu Z, Li Y, Lozada J, Pan J, Lin KS, Schaffer P, Perrin DM. J Labelled Compd Radiopharm. 2012; 55:491–496.(e) Liu Z, Li Y, Lozada J, Schaffer P, Adam MJ, Ruth TJ, Perrin DM. Angew Chem, Int Ed. 2013; 52:2303–2307.

6. (a) Liu Z, Hundal-Jabal N, Wong M, Yapp D, Lin KS, Benard F, Perrin DM. Med Chem Commun. 2014; 5:171–179.(b) Liu Z, Pourghiasian M, Radtke MA, Lau J, Pan J, Dias GM, Yapp D, Lin KS, Bénard F, Perrin DM. Angew Chem, Int Ed. 2014; 53:11876–11880.(c) Liu Z, Radtke MA, Wong MQ, Lin KS, Yapp DT, Perrin DM. Bioconjugate Chem. 2014; 25:1951–1962.(d) Pourghiasian M, Liu Z, Pan J, Zhang Z, Colpo N, Lin KS, Perrin DM, Bénard F. Biorg Med Chem. 2015; 23:1500–1506.(e) Liu Z, Chao D, Li Y, Ting R, Oh J, Perrin DM. Chem Eur J. 2015; 21:3924–3928. [PubMed: 25639468] (f) Wade CR, Zhao H, Gabbaï FP. Chem Commun. 2010; 46:6380–6381.(g) Li Z, Chansaenpak K, Liu S, Wade CR, Zhao H, Conti PS, Gabbaï FP. Med Chem Commun. 2012; 3:1305–1308.(h) Bernard J, Malacea-Kabbara R, Clemente GS, Burke BP, Eymin MJ, Archibald SJ, Jugé S. J Org Chem. 2015; 80:4289–4298. [PubMed: 25844635]

7. (a) Brahmi MM, Malacria M, Curran DP, Fensterbank L, Lacôte E. Synlett. 2013:1260–1262.(b) Arduengo AJ III, Davidson F, Krafczyk R, Marshall WJ, Schmutzler R. Monatsh Chem. 2000; 131:251–265.

8. Tian C, Nie W, Borzov MV, Su P. Organometallics. 2012; 31:1751–1760.

9. Khramov DM, Lynch VM, Bielawski CW. Organometallics. 2007; 26:6042–6049.

10. Lennox AJJ, Lloyd-Jones GC. J Am Chem Soc. 2012; 134:7431–7441. [PubMed: 22512340]

11. Liu S, Lin TP, Li D, Leamer L, Shan H, Li Z, Gabbaï FP, Conti PS. Theranostics. 2013; 3:181–189. [PubMed: 23471211]

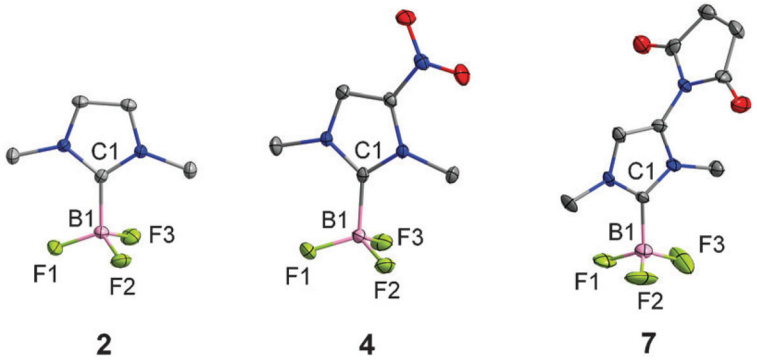

Fig. 1.

Crystal structures of the Arduengo carbene borane adducts **2**, **4**, and **7**. Ellipsoids are scaled to the 50% probability level and hydrogen atoms have been omitted for clarity.

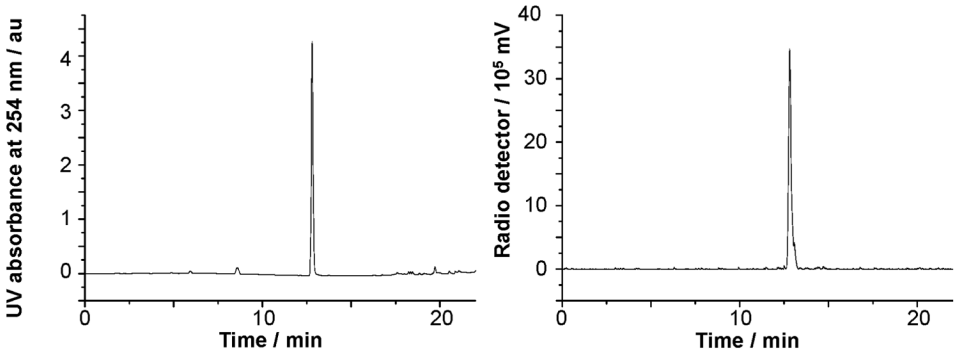

Fig. 2.

Left: UV trace of **7** as the standard reference. Right: Crude radio-HPLC profile for the ^{18}F-labeling of **7**.

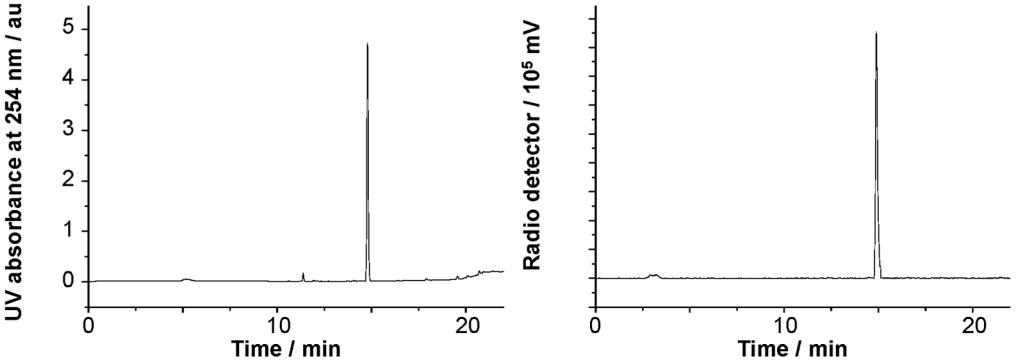

Fig. 3.

Left: UV traces of [^{18}F]**7**–H–Cys–Phe–OH as the standard reference. Right: Crude radio-HPLC profile for the ^{18}F-labeling of [^{18}F]**7**–H–Cys–Phe–OH.

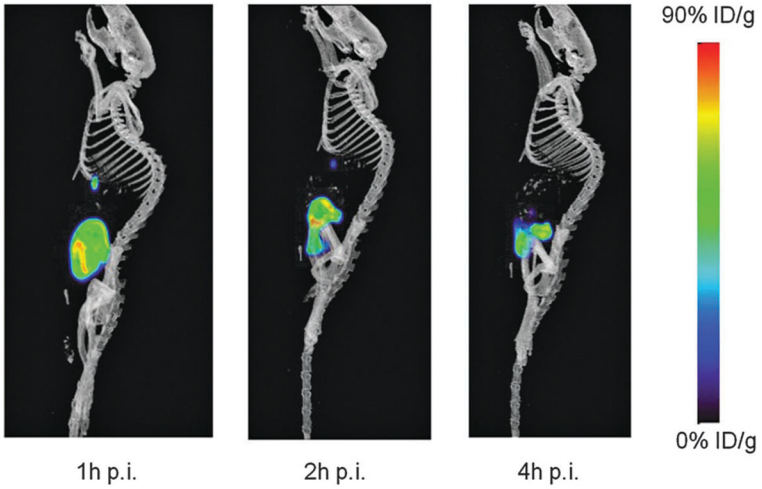

Fig. 4.

Decay-corrected whole-body microPET/CT sagittal images of a nude mice from a static scan at 1, 2 h and 4 h after injection of [^{18}F]**7**–H–Cys–Phe–OH.

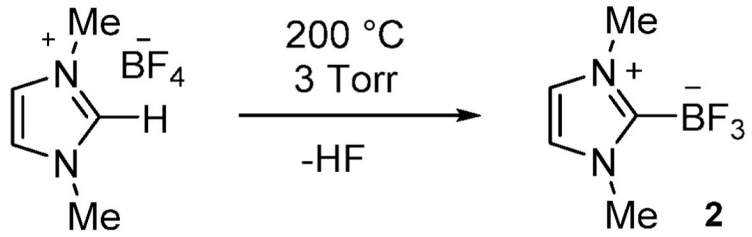

Scheme 1.
Synthesis of **2**.

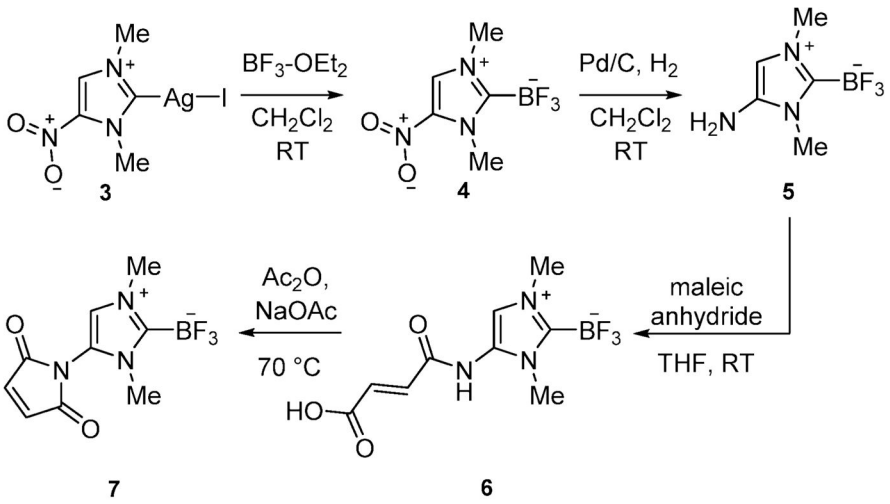

Scheme 2.

Synthesis of the maleimide derivative **7**.

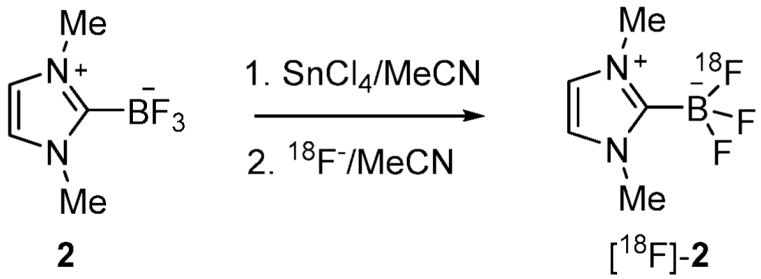

Scheme 3.

Scheme showing the radiolabeling of **2** *via* $SnCl_4$ assisted isotopic ^{18}F–^{19}F exchange.

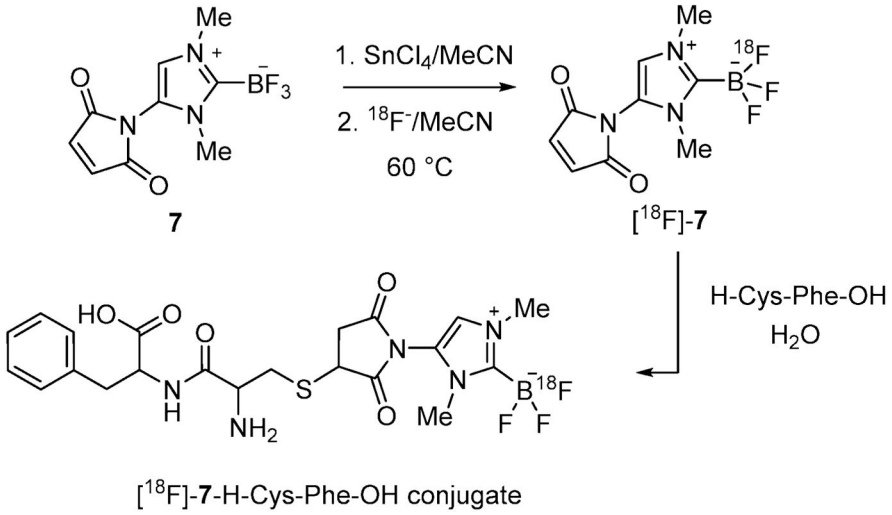

Scheme 4.

Scheme showing the preparation of the [^{18}F]**7**–H–Cys–Phe–OH conjugate.

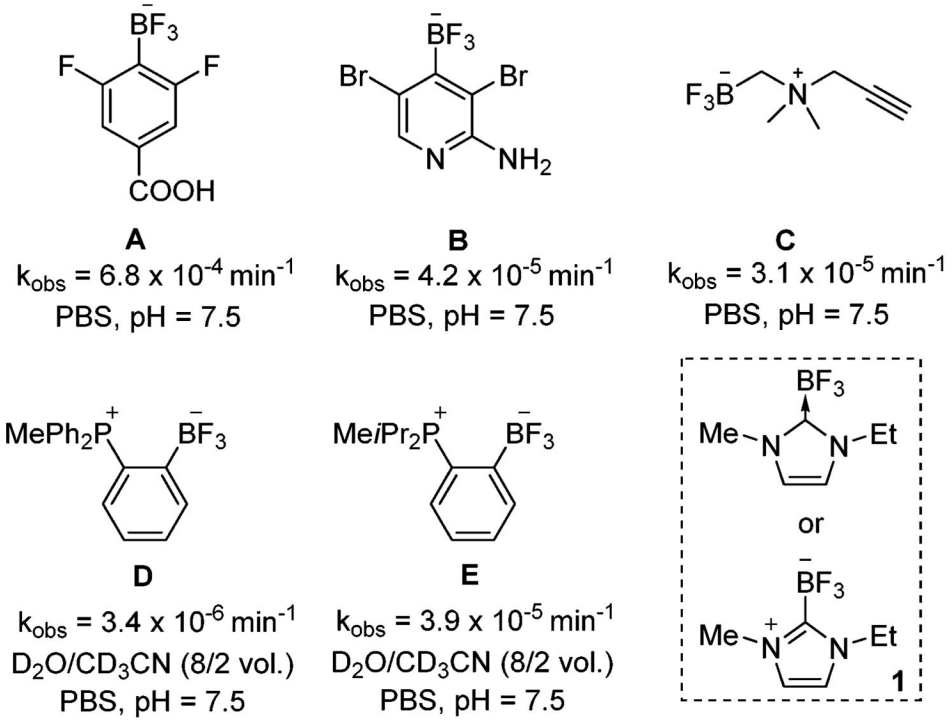

Chart 1.

Table 1

Radiosynthetic results for [^{18}F]**2**

Entry	[2] (mM)	$SnCl_4$ (equiv.)	Temp. (°C)	Time (min)	SA[a] (mCi μmol^{-1})	RCY[b] (%)
1	15	5	25	10	26.4	35.5
2	30	5	25	10	40.6	42.1
3	60	5	25	10	40.8	47.3
4	30	10	25	10	47.5	48.4
5	30	15	25	10	47.8	48.1
6	30	5	40	10	45.5	56.4
7	30	5	60	10	49.5	53.4
8	30	5	25	20	53.5	49.9
9	30	5	25	30	36.8	39.9

[a]Specific activity is determined by dividing the product activity by the amount of the product (based on the integration of UV-HPLC and compare with the UV chromatogram of the standard).

[b]RCY = activity of the isolated product/starting ^{18}F activity. All yields are decay corrected.